Supplementary Information for "Alternative Tree-Cover States of the Boreal Ecosystem: a Conceptual Model"

For Submission to Global Ecology and Biogeography

List of Supplementary Figures

List of Supplementary Tables

Introduction

This Supplementary text is intended as companion to the main manuscript and provides clarifications on methodology, results, and for the instances in which the main text refers to Supplementary Material. This document is structured as follows: each section corresponds to a reference in the main text. Each section contains additional information to what is provided in the manuscript and the details for the corresponding script that was originally used to obtain them.

1 Model coefficients

Model coefficients for all possible pairs of tree species (PFTs) are computed assuming the dynamical system (1) in Section 2.3 of the main text is in equilibrium, i.e., the three derivatives constituting the l.h.s. in (1) are all zero. With this assumption, the script produces a fitting of all the free coefficients and parameters in (1).

The fitting is performed with the *optimize.minimize* function of the *SciPy* package for python. The optimisation takes the r.h.s. of (1) as main function f and the l.h.s. as target function, using a truncated Newton (TNC) algorithm for the minimisation. To allow for small perturbations, as the ecosystem is never in perfect equilibrium, a small white noise is added to the target function, meaning the optimisation will try to minimise the value of f so that $f \sim 0$, but not exactly zero.

The main function f is evaluated over randomly sampled geographic gridcells over North America (where the tree-species details are available); f takes as input the proportions between the two selected tree species (*spec1* and *spec2*) and the environmental conditions linked to the specific gridcells, namely Growing degree days above 0 °C (GDD0) for the growth functions r_i, and Soil moisture (SM), Permafrost distribution (PZI), and Mean rainfall (MAR) for the carrying capacities K_i.

Note that environmental conditions do not affect the value of the optimised competition coefficients, as these are based uniquely on the proportions of tree species. Furthermore, r_i and K_i are here calculated as polynomial functions of the environmental variables, and the optimisation determines only the coefficients of the polynomials. This is done so that the results of the optimisation can be applied and tested in regions which are independent from the original random sample, e.g., Eurasia, which is not covered by the tree-species dataset.

Finally, the results of the optimisation are applied to multistable gridcells over both North America and Eurasia to obtain the model coefficients. In doing this, the competition coefficients are fixed using values from the optimisation, whereas the values of r_i and K_i are determined using the polynomial coefficients resulting from the optimisation, together with the values of the environmental conditions over the multistable gridcells. When running the model after calibration, only gridcells for multistable areas are used. This means that in Eurasia all model results are out-of-sample, whereas in North America results are a mixture of in- and out-of-sample gridcells is used, as the calibration is performed with random sampling from the entire areas where the different plant functional types are present. Furthermore, the calibration of coefficients does not include any information on the total tree-cover fraction distribution, which is then the main variable evaluated from model results. It is also important to note that, even though calibration of coefficients is performed only over North America, all the relevant plant functional types are present. In fact, other than Avoiders and Resisters, the Canadian dataset contains a (albeit small) population of Resisters exhibiting fire-resisting adaptations comparable to those of Eurasian Resisters, i.e., dropping needles (deciduous conifer), absence of low branches, thick bark (see, for instance, Rogers et al. (2015); Beaudoin et al. (2014); Wirth (2005); Arno & Fischer (1995); Scher (2002)). This allows to calibrate the parameters for the three major fire plant functional types and run the model in both North America and Eurasia.

These computations can be reproduced using the Jupyter/IPython notebook

00_Paper_Competition_Coefficients_Eurasia_Larix_Picea.ipynb.

To run the file, it is sufficient to select the tree species to use. To do so, in the second cell, initialise the two variables *spec1* and *spec2* to one of the following values: 0 for *Abies*, 1 for *Larix*, 2 for *Picea*, 3 for *Pinus*, 4 for *Broadleaf*. To save the results, set the value of the variable *math_add* to the desired output address. All the files necessary to run the script are already included in the Supplementary Material folder.

Model simulations are then performed in Mathematica. The problem is implemented as a system of differential equations solved numerically with NDSolve. Additionally, temporal variations for the stochastic variables affects the system. These variations include nitrogen availability, which fluctuates as a Uniform random variable affecting the carrying capacities, and stochastic disturbances, modelled as a Bernoulli distributed process, modulated with a random uniform variable in the case of resister trees, and doing always maximum damage with avoider and embracer trees. Scripts to perform these simulations are provided in the folder *Supplementary_Mathematica*, divided in Landsat and Modis based on the remotely-sensed TCF values used. Simulations' results are collected in the folder *Supplementary_Python/Dataset/Model_tcf* and are plotted with python via the script

04_Paper_Plot_Tree_Competition_Histograms_and_Multistable_Division_and_Species_Evolution.ipynb

1.1 Density dependent term

As part of our analysis, we tested whether the inclusion of a density dependent term in the model equations would alter its dynamics in terms of multistability and multimodality. To do so, we performed simulations and model analysis as reported in the manuscript, but with a model that includes a density-dependent term, namely A_i. The equations are then as follows, with all terms except A_i as in the manuscript.

$$\begin{aligned}\frac{\mathrm{d}x_1}{\mathrm{d}t} &= r_1(\mathrm{g})x_1C_1(x_1,x_2,x_3) - A_1(x_1,x_2) - D_1(x_1)\xi(t)\\ \frac{\mathrm{d}x_2}{\mathrm{d}t} &= r_2(\mathrm{g})x_2C_2(x_1,x_2,x_3) - A_2(x_1,x_2) - D_2(x_2)\\ \frac{\mathrm{d}x_3}{\mathrm{d}t} &= r_3(\mathrm{g})x_3C_3(x_1,x_2,x_3) - D_3(x_3)\end{aligned} \tag{1}$$

In our sensitivity-analysis, the density-dependent term A_i, can either correspond to a positive density dependence, a negative density dependence, or be zero (the latter corresponding to the main text). Thus, A_i can either represent the Allee effect, simulating hence a lack of protection from established trees to seedlings (Holmgren et al., 1997; Rietkerk & van de Koppel, 1997; Van Nes et al., 2014), causing a net reduction of growth at low tree-cover densities and declining at higher tree-cover densities; or a negative density dependence, due to shared natural enemies or strong competition for resources, which causes a reduction of individuals that are surrounded by neighbours of the same species (Comita et al., 2010; Mangan et al., 2010). These phenomena are particularly relevant in highly diverse communities such as tropical forests, where a recent analysis has shown that the most common species are those whose seedling survival is minimally affected by the local density of neighbours (Comita et al., 2010). By contrast, the boreal forest is composed of only a few plant functional types, which have to be considered common. In agreement with (Comita et al., 2010), our density-dependent term has a smaller effect than direct competition between PFTs and fire disturbances. Furthermore, our analysis shows that the density-dependent term does not influence the dynamics of the model when it comes to multistability, i.e., the number of stable equilibria is unaffected, and the density term only adds slight modulations to the location of the main peaks in the final tree-cover fraction distribution, as reported in Fig. S1. Finally, Table S1 reports the results of K-sample Anderson-Darling tests (Scholz & Stephens, 1987) verifying the hypothesis that modelled and observed tree-cover fraction can be considered as coming from the same distribution.

2 Greening trends

The analysis of LAI and NDVI trends is performed using the Jupyter/IPython notebook

01_Paper_greening_trends_comparison.ipynb.

A summary of the analysis regarding Mutual Information for Clusters, and the distribution of LAI and NDVI trends is depicted in Fig. S2. The first part of the script simply loads a few datasets containing:

- the LONLAT coordinates of the multistable gridcells;
- the values of LAI and NDVI trends over multistable gridcells;
- an identifier for each multistable gridcell referring to the environmental variables underlying it;
- the value of the tree-cover fraction (TCF) over the multistable gridcells.

After loading these datasets and defining a few plotting functions, the script computes the value of several measures in each geographic zone (*ea_e, ea_w, na_e, na_w*). To be able to compute measures properly, a

Table S1: *K-sample Anderson-Darling (AD) tests verifying the hypothesis that modelled and observed tree-cover fraction can be considered as coming from the same distribution in terms of alternative stable states. Goodness-of-fit results are related either to binned data (with 10% bins), or to the categorised alternative states (CAS) of tree cover, i.e., divided into treeless, open woodland, and forest states. Data include simulations performed using a positive density term (PDE TCF), a negative term (NDE TCF), a null term (ZDE TCF), and the observed tree-cover fraction distribution (TCF). Critical values are for the 25%, 10%, 5%, 2.5%, 1% significance levels, respectively.*

Data	K-sample AD test values	Critical values
Binned TCF - ZDE TCF	0.0197	0.325, 1.226, 1.961, 2.718, 3.752
Binned NDE TCF - ZDE TCF	0.0197	0.325, 1.226, 1.961, 2.718, 3.752
Binned ZDE TCF - PDE TCF	-0.8672	0.325, 1.226, 1.961, 2.718, 3.752
Binned NDE TCF - PDE TCF	-0.8672	0.325, 1.226, 1.961, 2.718, 3.752
CAS TCF - ZDE TCF	-0.8672	0.325, 1.226, 1.961, 2.718, 3.752
CAS NDE TCF - ZDE TCF	-0.8672	0.325, 1.226, 1.961, 2.718, 3.752
CAS ZDE TCF - PDE TCF	-0.5124	0.325, 1.226, 1.961, 2.718, 3.752
CAS NDE TCF - PDE TCF	0.0197	0.325, 1.226, 1.961, 2.718, 3.752

reference case is created, using a random sample of the same size of the total multistable area for the zone of interest, as described in the main manuscript in Section 2.2. Several measures and tests are performed, as reported in Tables S2, S3, and S4.

MI is a measure that quantifies the amount of information, in the sense of Information Theory (Vinh et al., 2010), shared between clusterings, i.e., segmentations of a set of elements into subsets with similar properties (in this case similar greening trends and similar environmental conditions). MI values close to zero signify that there is no link between the conditions causing multistable states and greening trends. On the opposite, values close to one indicate that there is an almost complete overlap in the conditions determining the vegetation state and the greening trends. Spearman's rank-order correlation coefficients (r_s) assess how well the relationship between two variables can be described using a monotonic function, whereas Kendall's rank correlation coefficients (τ) evaluate the similarity of the orderings of the data when ranked by each of the quantities. Of the three measures, τ and r_s only assess the monotonicity and ordering of the relationship, whereas MI is able to capture the shared information between the two clusters, and it is therefore the more complete and informative of these measures.

Table S2: *Complete table containing Mutual Information (MI) for clusters calculated using trends in Leaf Area Index (LAI) and Normalised Difference Vegetation Index (NDVI) against environmental conditions determining alternative tree-cover states (ATS) computed over multistable regions. As can be seen from the corresponding information in Fig. S2, trends in multistable areas in North America are either close to zero or non-significant, so they were excluded from the main manuscript. Note that reference values may vary slightly due to the random sampling. Values in parentheses represent the difference in percentage between the reference and multistable case.*

Region	MI(LAI, ATS)		MI(NDVI, ATS)	
	Ref	Multistable	Ref	Multistable
Eastern Eurasia	0.43	0.10 (76%)	0.42	0.18 (56%)
Western Eurasia	0.50	0.13 (73%)	0.53	0.09 (82%)
Eastern North America	0.14	0.04 (63%)	0.18	0.03 (83%)
Western North America	0.16	0.00 (99%)	0.25	0.00 (99%)

Table S3: *Complete table for Spearman's rank-order correlation coefficients (r_s) measuring monotonic association between LAI trends (LAI) and environmental conditions determining alternative tree-cover states (ATS), and between NDVI trends (NDVI) and ATS, over multistable regions.*

Region	r_s(LAI, ATS)	r_s(NDVI, ATS)
Eastern Eurasia	-0.06	0.19
Western Eurasia	-0.29	-0.28
Eastern North America	-0.08	0.005
Western North America	nan	nan

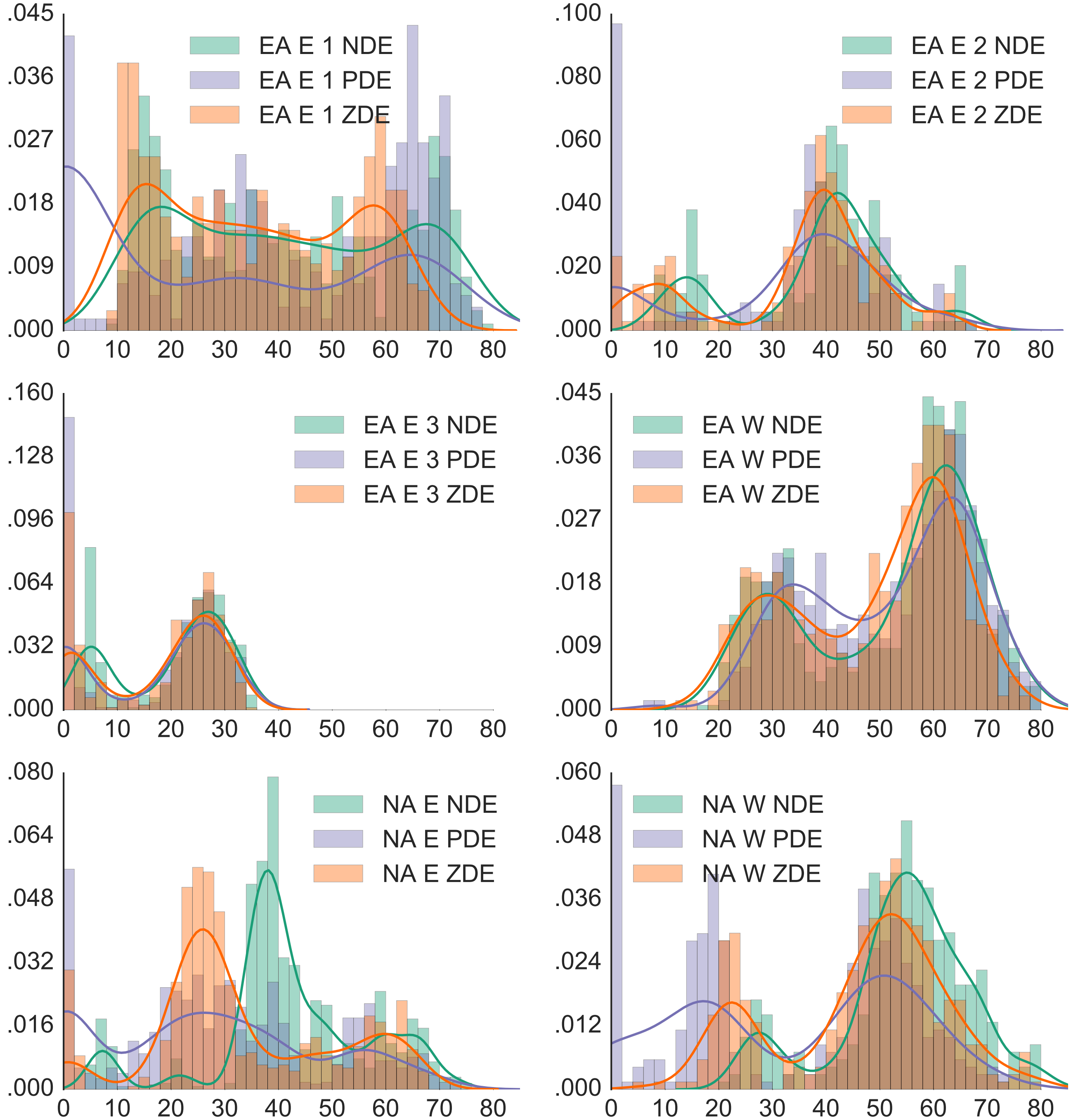

Figure S1: *Plots showing the modelled tree-cover fraction distributions using positive density dependence (PDE), a negative density dependence (NDE), or null density dependence (ZDE).*

Table S4: *Complete table for Kendall's rank correlation coefficients (τ) measuring ordinal association between LAI trends (LAI) and environmental conditions determining alternative tree-cover states (ATS), and between NDVI trends (NDVI) and ATS, over multistable regions.*

Region	τ(LAI, ATS)		τ(NDVI, ATS)	
	Ref	Multistable	Ref	Multistable
Eastern Eurasia	0.08	-0.04	-0.05	0.14
Western Eurasia	0.13	-0.26	-0.01	-0.25
Eastern North America	-0.19	-0.07	-0.17	-0.005
Western North America	0.20	nan	0.18	nan

MODIS Trends 2000–2015 LAI & NDVI Comparison with Transition Zones from Abis & Brovkin 2017

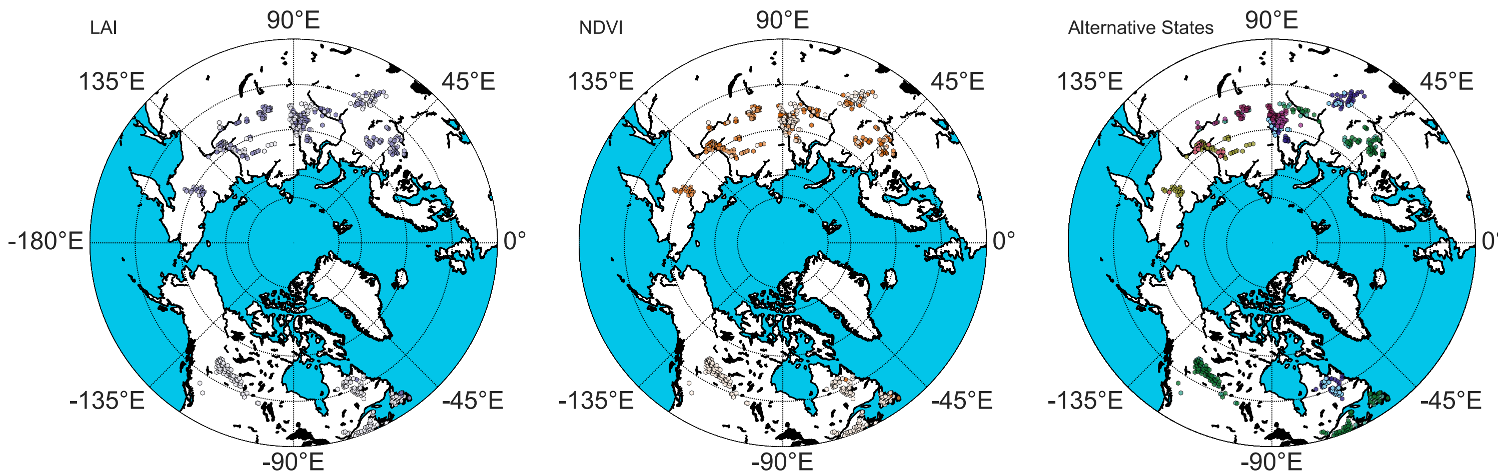

Mutual Information for Clusters

Region	MI(LAI,CLASS) Random	MI(LAI,CLASS) Transition	Difference	MI(NDVI,CLASS) Random	MI(NDVI,CLASS) Transition	Difference
East North America	0.108617	0.040627	**-62,6%**	0.116088	0.035303	**-69,6%**
West North America	0.168539	0.000028	**-99,9%**	0.260792	0.000028	**-99,9%**
East North Eurasia	0.426407	0.101625	**-76,2%**	0.416893	0.182744	**-56,2%**
West North Eurasia	0.505054	0.135029	**-73,3%**	0.525624	0.094677	**-81,9%**

Figure S2: *Plots represent, from left to right, the distribution of LAI trends, NDVI trends, and alternative tree-cover states. LAI and NDVI trends are shaded according to the intensity of the trend, white being null or non-significant trend, deep purple or orange meaning high trend values. Colours for alternative states are as in Abis & Brovkin (2017) and describe the current tree-cover state of the gridcell. The table reports values of the Mutual Information for Clusters (MI) obtained in the reference and multistable cases, over each region, using one of the two trend values together with CLASS, which represents the environmental conditions of the gridcell.*

3 Stability of equilibria

The stability of the equilibria of the model is evaluated numerically in Maple 2015. All Maple scripts can be located in the folder *Supplementary_Maple*, and are of two types: those to determine the number of equilibria of the model as a dynamical system, and those to determine the stability of said equilibria. Each script can be simply run by adjusting the initial address of the folder */Supplementary_Python/Datasets/Model_Parameters/Modis_param/*, where the coefficients of the optimisation procedure of Section 1 are stored.

To evaluate the stability of an equilibrium, the Jacobian matrix of the system is computed, and it is evaluated at the equilibrium point. The Jacobian matrix of a system of Ordinary Differential Equations (ODEs) is the matrix of the partial derivatives of the right-hand side with respect to state variables, where all the derivatives are evaluated at the equilibrium point. Its eigenvalues determine linear stability properties of the equilibrium; in particular, an equilibrium is asymptotically stable if all eigenvalues have negative real parts, and it is unstable if at least one eigenvalue has positive real part (Kuznetsov, 2013).

From the ecological point of view, it is of interest when multiple stable equilibria exist, or when bifurcations happen. A bifurcation occurs when a small smooth change made to the parameter values (the bifurcation parameters) of a system causes a sudden qualitative or topological change in its behaviour, for instance a change in the number of stable equilibria, or a phenomenological change in the nature of the equilibria (Kuznetsov, 2013; Rasmussen, 2015).

The Maple scripts provided, first calculate the equilibria of the dynamical system in all multistable gridcells, and then use these equilibria to evaluate the sign of the real part of the Jacobian's eigenvalues. Only the stable equilibria are kept and listed together with the parameters they are associated to, and the proportions of tree species at equilibrium. Results cannot be summarised in a table, as they are too lengthy. Their qualitative description is reported in the main text. To access the full list of stable equilibria, it's sufficient to open the files in the *Supplementary_Maple* folder, named

#NN_Paper_Stability_#Region_#Product.mw

where *#NN* is a number in 06–21, *#Region* is the geographic region, following the names

$$EA\_E\_1, EA\_E\_2, \dots, NA\_W,$$

and *#Product* is either *Modis* or *Landsat*. Data are already saved, so compilation is not necessary to only visualise results.

4 Differences in environmental conditions between continents

To run the model in explicit geographical locations, we force it with environmental conditions from observations, as in Table 1. The distributions of these variables are similar within the two continents, as can be seen in Fig. S3, but there are differences between the multistable areas and within subregions which produce the different multimodal distributions discussed in the manuscript. In particular, the percentage of areas underlain by permafrost is greater in Eurasia than in North America, as can be seen by the asymmetric distributions of PZI in Fig. S3, especially in multistable areas.

4.1 Permafrost

The folder *Supplementary_Maple* contains two additional files, *22_Paper_PZI_Bifurcation.mw* and *23_Paper_PZI_Comparison_stability.mw*. These files contain plots of the number and location of stable equilibria of the dynamical system in phase space when varying the permafrost conditions, i.e., using values for PZI from Eurasia in North America and vice versa, while keeping the other environmental variables to

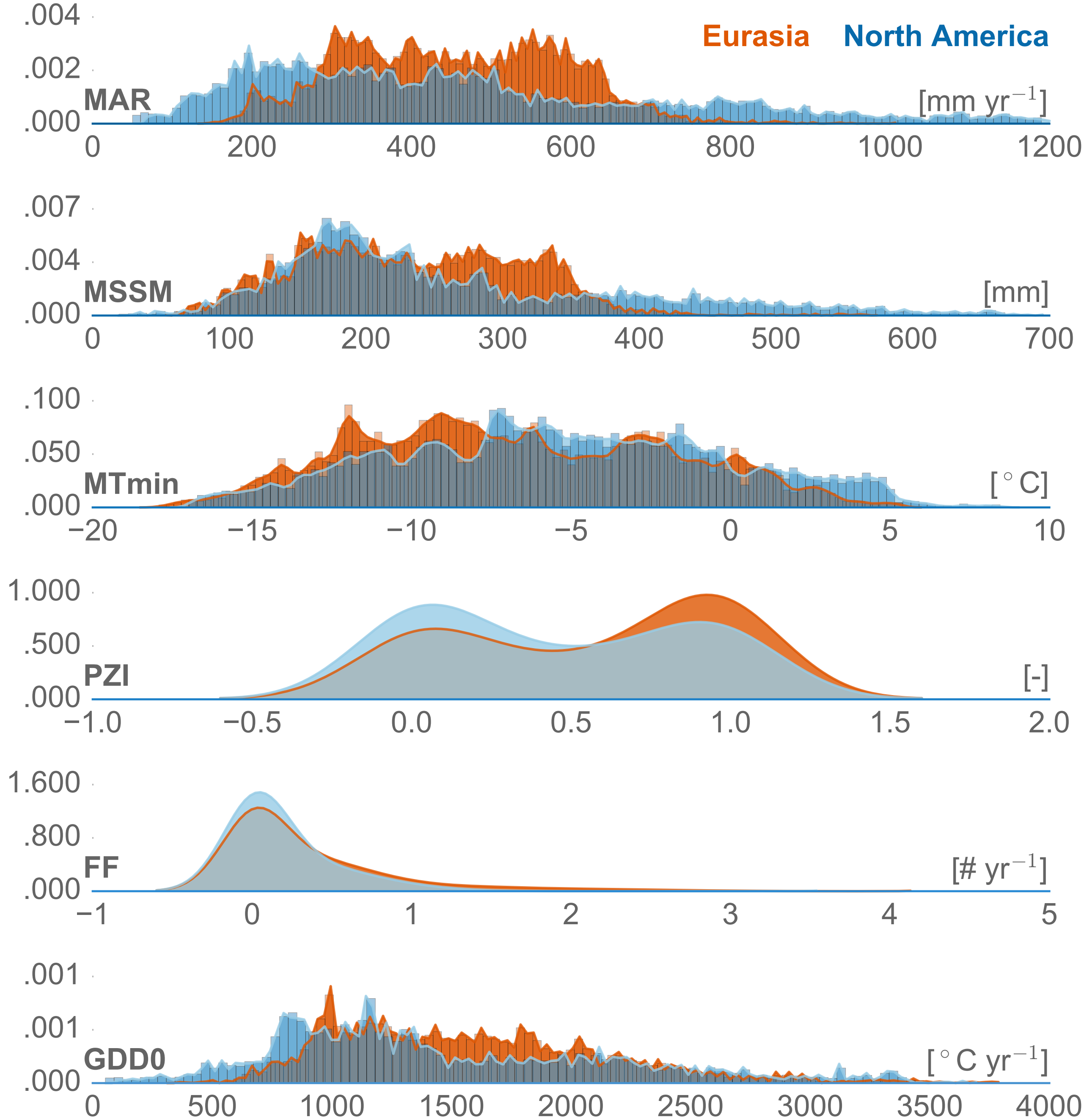

Figure S3: *Plots showing the distributions of the main environmental variables in North America and Eurasia.*

their original values. In particular, *22_Paper_PZI_Bifurcation.mw* contains two main plots (the first two) visualising the number of stable equilibria (y-axis) versus the presence of permafrost (x-axis). The first plot is for North America with original PZI conditions, and shows the passage from one to two stable equilibria. The second plot makes use of PZI from Eurasia, and shows passages from one to two to three stable equilibria. The rest of the file shows how the parameters vary when changing PZI only, and how this affects the dynamics of the system with respect to the analysis showed in Fig. 5 of the manuscript. A summary of this analysis is reported in the following figures. In particular, Figure S5 depicts how the permafrost conditions from Eurasia push Embracers in a phase-space area where only the trivial null equilibrium is present, while Resisters can remain in different stable states. To properly assess this plot, it is necessary to combine it with the information provided by Figure S4, which shows how the number of stable equilibria of the model in North America depends on PZI.

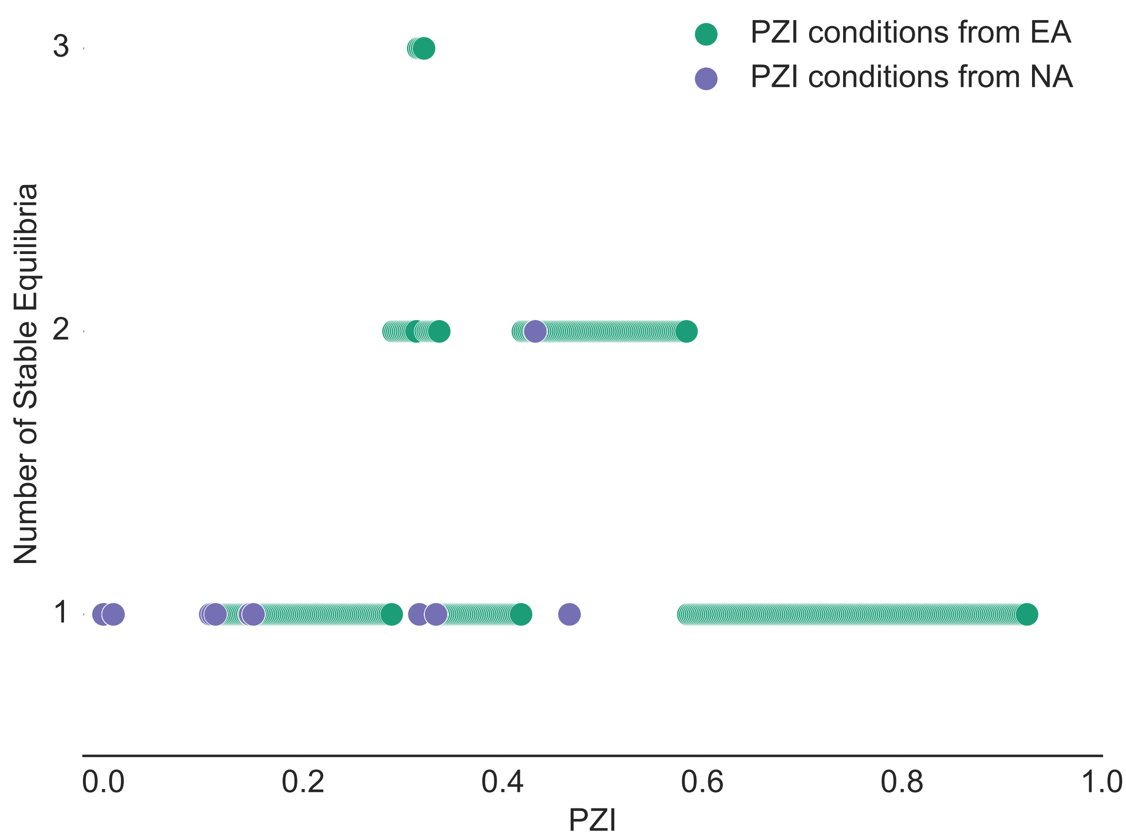

Figure S4: *Plots showing the relationship between PZI, on the x-axis, and the number of stable equilibria of the model in North America, on the y-axis. Purple circles correspond to standard present-day conditions for North America. Green circles make use of present-day environmental conditions for North America with the exception of permafrost conditions which are from Eurasia.*

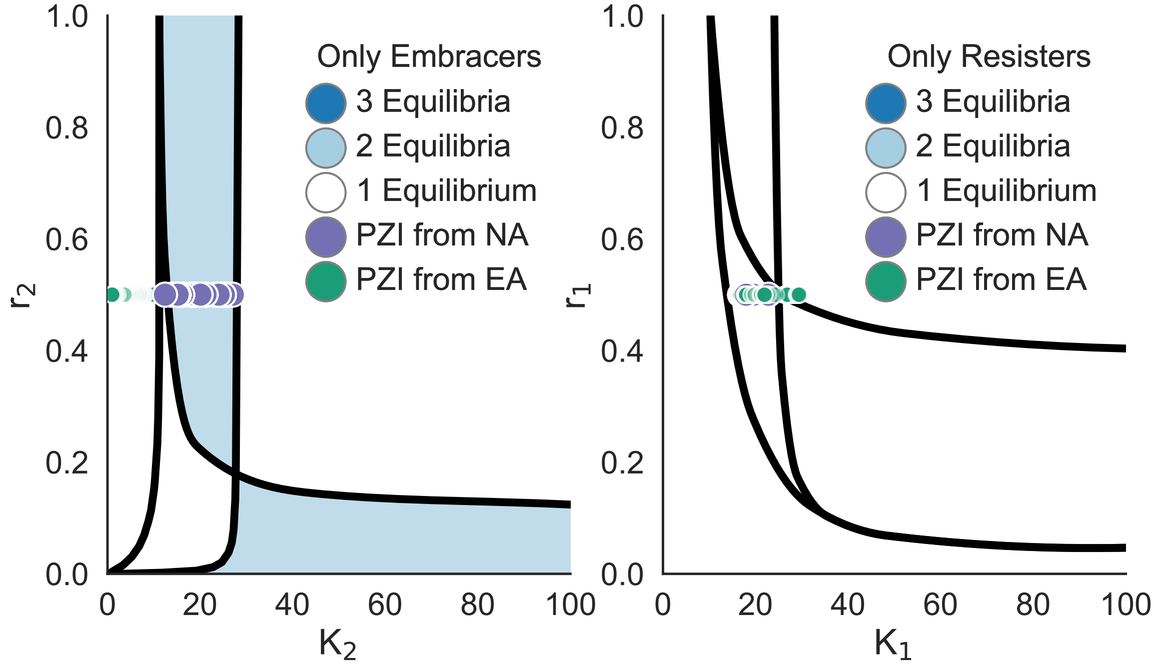

Figure S5: *Plots showing how the permafrost conditions affect the positioning of the system in the parameters phase space related to the number of equilibria of the model. Purple circles correspond to standard present-day conditions for North America. Smaller green circles make use of present-day environmental conditions for North America with the exception of permafrost conditions which are from Eurasia.*

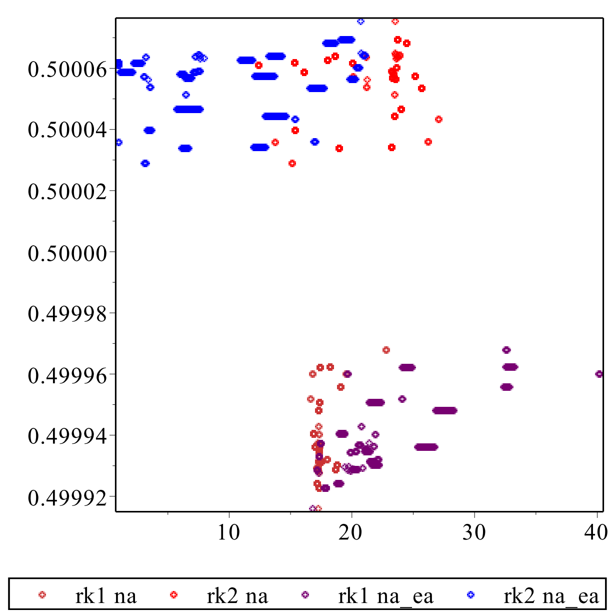

Figure S6: *Plot showing how the permafrost conditions affect the growth functions and carrying capacities of the system. The suffix _na_ea indicates permafrost conditions from Eurasia used in North America, whereas _na indicates original conditions for North America.*

References

Abis, B. & Brovkin, V. (2017). Environmental conditions for alternative tree-cover states in high latitudes. *Biogeosciences*, *14*(3), 511–527. Retrieved from https://www.biogeosciences.net/14/511/2017/ doi: 10.5194/bg-14-511-2017

Arno, S. F. & Fischer, W. C. (1995). Larix occidentalis: fire ecology and fire management. *US Dept. of Agriculture, Forest Service, Intermountain Research Station*.

Beaudoin, A., Bernier, P., Guindon, L., Villemaire, P., Guo, X., Stinson, G., ... Hall, R. (2014). Mapping attributes of canada's forests at moderate resolution through k nn and modis imagery. *Canadian Journal of Forest Research*, *44*(5), 521–532.

Comita, L. S., Muller-Landau, H. C., Aguilar, S. & Hubbell, S. P. (2010). Asymmetric density dependence shapes species abundances in a tropical tree community. *Science*, *329*(5989), 330–332.

Holmgren, M., Scheffer, M. & Huston, M. A. (1997). The interplay of facilitation and competition in plant communities. *Ecology*, *78*(7), 1966–1975.

Kuznetsov, Y. A. (2013). *Elements of applied bifurcation theory* (Vol. 112). Springer Science & Business Media.

Mangan, S. A., Schnitzer, S. A., Herre, E. A., Mack, K. M., Valencia, M. C., Sanchez, E. I. & Bever, J. D. (2010). Negative plant–soil feedback predicts tree-species relative abundance in a tropical forest. *Nature*, *466*(7307), 752.

Rasmussen, M. (2015). Bifurcations of random dynamical systems. *Banff International Research Station for Mathematical Innovation and Discovery*.

Rietkerk, M. & van de Koppel, J. (1997). Alternate stable states and threshold effects in semi-arid grazing systems. *Oikos*, 69–76.

Rogers, B. M., Soja, A. J., Goulden, M. L. & Randerson, J. T. (2015). Influence of tree species on continental differences in boreal fires and climate feedbacks. *Nature Geoscience*, *8*(3), 228–234. Retrieved from http://www.nature.com/doifinder/10.1038/ngeo2352 doi: 10.1038/ngeo2352

Scher, J. S. (2002). Larix occidentalis. *Fire Effects Information System*. Retrieved from https://www.fs.fed.us/database/feis/plants/tree/larlya/all.html (U.S. Department of Agriculture, Forest Service, Rocky Mountain Research Station, Fire Sciences Laboratory)

Scholz, F. W. & Stephens, M. A. (1987). K-sample anderson–darling tests. *Journal of the American Statistical Association*, *82*(399), 918–924.

Van Nes, E. H., Hirota, M., Holmgren, M. & Scheffer, M. (2014). Tipping points in tropical tree cover: Linking theory to data. *Global Change Biology*, *20*(3), 1016–1021. doi: 10.1111/gcb.12398

Vinh, N. X., Epps, J. & Bailey, J. (2010). Information theoretic measures for clusterings comparison: Variants, properties, normalization and correction for chance. *Journal of Machine Learning Research*, *11*(Oct), 2837–2854.

Wirth, C. (2005). Fire regime and tree diversity in boreal forests: implications for the carbon cycle. In *Forest diversity and function* (pp. 309–344). Springer.